University of Glasgow
DEPARTMENT OF
AEROSPACE
ENGINEERING

USE OF A NUMERICAL MODEL IN THE CONCEPTUAL DESIGN OF A NEW BLADE VORTEX INTERACTION FACILITY

By

C.M. Copland , F.N. Coton , R.A.McD. Galbraith

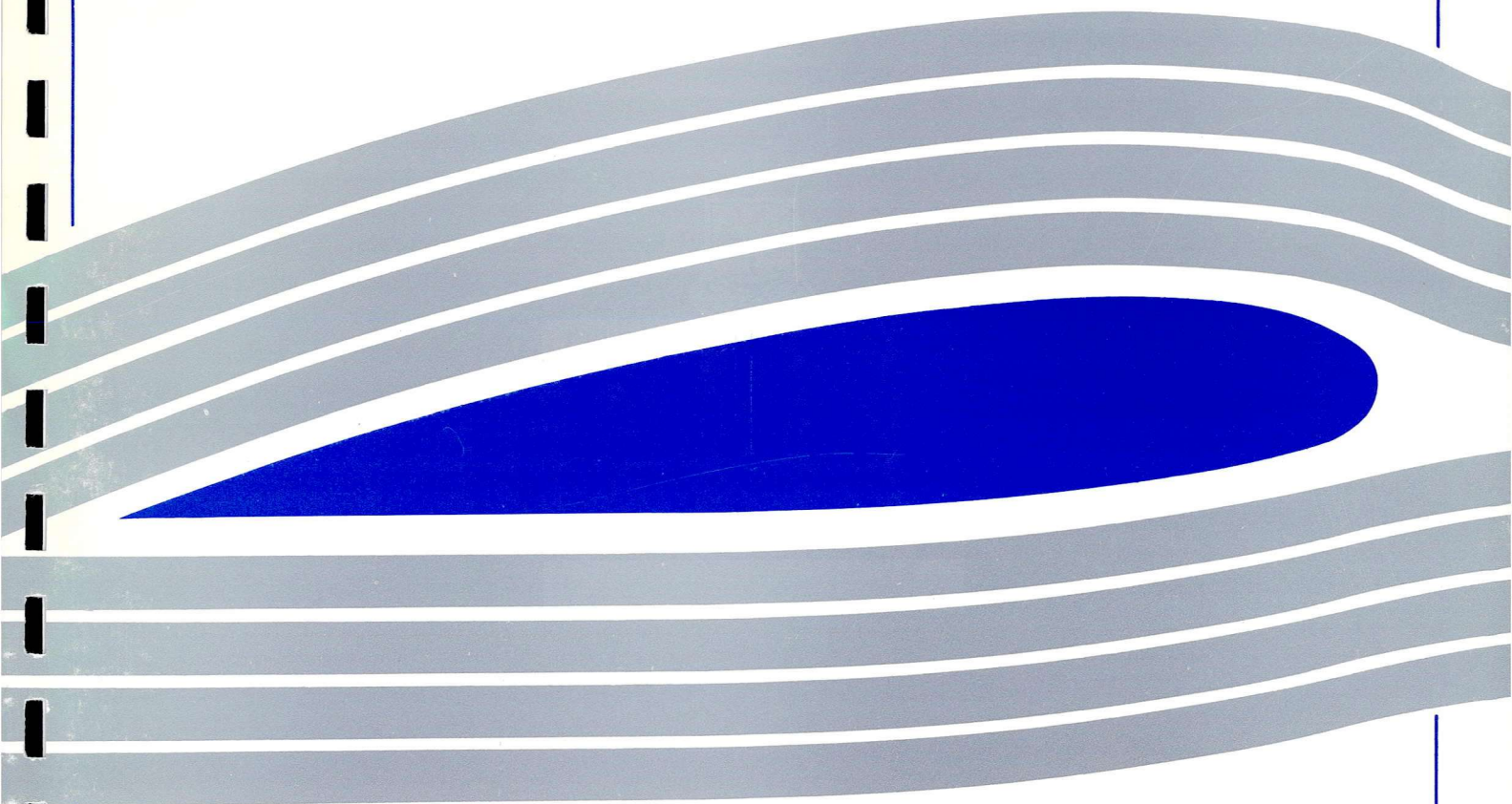

USE OF A NUMERICAL MODEL IN THE CONCEPTUAL DESIGN OF A NEW BLADE VORTEX INTERACTION FACILITY

By

C.M. Copland , F.N. Coton , R.A.McD. Galbraith

University of Glasgow

Department Of Aerospace Engineering

Internal Report Number 9509

Contents

Nomenclature

AOA1	Geometric angle of incidence at ALP1
AOA2	Geometric angle of incidence at ALP2
c	Rotor chord length
R	Rotor tip radius
X,Y	Position of rotor axis in wind tunnel coordinate system
Start Azi	Rotor start azimuth
AZI1	Rotor position at end of initial acceletation
AZI2	Rotor position at end of second acceleration or constant velocity phase.
Stop Azi	Rotor position at end of deceleration phase
Start Alp	Rotor position for start of pitch up
ALP1	Rotor position with incidence at AOA1
ALP2	Rotor position with incidence at AOA2
Stop Alp	Rotor position for end of pitch down
WS Vel	Working Section Velocity
TV1	Specified tip velocity at AZI1
TV2	Specified tip velocity at AZI2
tmax	Maximum time of simulation
tstep	Time step during simulation
nplot	Number of wake plots

Summary

This report describes and presents results from a numerical model developed to aid the preliminary design of a new wind tunnel based blade-vortex interaction (BVI) facility. The proposed facility will simulate tail rotor BVI by interacting a transverse vortex, produced by a single-bladed rotor situated in the wind tunnel contraction, with a blade mounted vertically in the tunnel working section. In the model a three dimensional source panel method is used to calculate the constrained flow through the low speed wind tunnel and a free wake vortex model represents the wake generated by the upstream rotor. Convection of the wake is then determined by superposition of the undisturbed tunnel velocity and the induced velocity components from the wake itself. Results, obtained via a parametric analysis, illustrate the geometry of the wake and tip vortex and their relation to basic design parameters. In particular, two possible operational strategies for the upstream rotor are examined with reference to developement of the experimental facility. It is concluded that, while a short duration finite rotor traverse may be the optimum vortex generation strategy, a continuous running rotor may be the most cost effective option.

Introduction

The flow field around modern rotor craft is both highly complex and unsteady. Of considerable importance are the concentrated trailed tip vortices generated by the main rotor which may convect and interact with the other rotor blades, the tail rotor and the fuselage. In powered descent and vigorous manoeuvring these interactions become more distinct with the result of unwanted phenomena such as noise, vibration and, in the case of interactions with the tail rotor, unusual yaw handling and control problems. The need to reduce these effects requires a clear understanding of the fundamental fluid dynamic characteristics of blade-vortex interactions.

In certain flight cases the main rotor will experience multiple vortex interactions which occur when a main rotor blade interacts with the tip vortex of a preceding blade. The angle of the interactions varies from near parallel through what is commonly termed oblique interactions to near perpendicular. These interactions are all characterised by the interacting vortex lying in a plane parallel to the plane of the blade. This is not the case, however, with main rotor tip vortex /tail rotor interactions when the interacting vortex lies in a plane perpendicular to that of the blade. Experimental research has, to date, targeted the problem of interactions on the main rotor blade but there is currently a considerable dearth of information on interactions associated with the tail rotor environment.

A number of experimental studies have been carried out into the fundamental mechanism for a vortex approaching a rotating blade. In this respect the studies conducted by Surendraiah[1] and subsequently Padakannaya [2] using an upstream wing tip to generate a vortex that interacted with a downstream rotor are seminal work. This work enabled the gross features of the blade-vortex interaction to be illustrated. Researchers at NASA Ames[3] developed this approach further in the

eighties using a similar facility but with better resolution in the pressure data allowing a "convective disturbance" in the airfoil pressure distribution to be identified. Further studies at Glasgow University [4-6] improved on previous pressure and aerodynamic load measurements but also provided vital flow field information through the use of Particle Image Velocimetry (PIV). The PIV results provided high quality images of the local blade flow field at various stages of the interaction process.

In wind tunnel tests of a model MBB BO-105 rotor Van der Wall [10] successfully measured the pressure distribution around one instrumented rotating blade of a complete rotor system to concentrate on BVI locations and noise radiation. Test were conducted in high and low speed cases representing descent flight conditions with a high noise level. The low speed BVI case was characterised by very strong vortex interactions at the blade tip which produce an extreme noise producing state commonly known as blade slap. This enabled the BVI locations for the complete rotor to be determined and then comparison drawn to the aerodynamic lift and moment distributions. Whilst not concentrating on the fundamental fluid dynamic aspect of BVI, the study identified that, in the full rotor environment, many blade vortex interactions involve pairs of trailed vortices. These pairs of voritices occur on the advancing side of the rotor, rotating in different directions, in the high speed case. There is still a need for continued research into twin vortex interactions as, at present, only the mechanism for the generation has been noted and not the detailed influence on the local blade flowfield and noise radiation.

Other studies have used different experimental set-ups to investigate the fundamental aspects of blade vortex interactions, notably Seath et al. [7] and Straus et al. [8]. In these tests the pitching motion of an upstream aerofoil generated a nominally two-dimensional shed vortex which convected downstream to interact with a second (fixed) airfoil. These test do have the advantage of varying the orientation of the fixed blade enabling the vortex line to line to lie either perpendicular or parallel to the

blade surface. However, it is doubtful whether the structure of the shed vortex comprehensively mimics that of the trailing tip vortex of a main rotor.

Unfortunately there hve been few experimental studies conducted on main rotor /tail rotor interactions. Most notible was the in-flight study carried out by Ellin [11] on the DRA Research Lynx with an instrumented tail rotor designed to obtain pressure data. This study noted six distinct regions of main rotor/tail rotor interaction each corresponding to a different mechanism in the low speed envelope. The tests were carried out in hover, forward flight and in what is commonly termed quartering flight. Ellin stated that further experimental work was required into blade vortex interaction with the vortex perpendicular to the blade surface to investigate these phenomena.

Obviously, rotorcraft flight testing is an expensive and, to most, inaccessible method of examining tail rotor interaction. Consequently, wind tunnel based studies may provide the most appropriate means of enhancing contemporary understanding of BVI. The crucial factor in all experiments to date has been the manner in which the interacting vortices have been generated and their subsequent trajectory through the wind tunnel's working section. It is essential that the detailed structure of the interacting vortex and the vortex trajectory, its stability and tendency to "wander" from its mean path are known. This applies irrespective of the method of generation of the vortex.

The present study is primarily concerned with the design of a facility for the generation of a transverse trailed tip vortex in a low speed wind tunnel. The facility will consist of a single-bladed rotor positioned in the contraction of a low speed wind tunnel. The design of the experimental facility is in progress at present and a numerical model has been developed to assist. In particular the model has been used to determine the convection and geometry of the wake and related tip vortex produced by the rotor as they progress through the working section. The computational model

and selected results are discussed and related to the practical development of the new BVI facility. This facility, once developed, could be used to investigate fundamental aspects of many different vortex interactions but, in particular, interactions where the vortex orientation is perpendicular to a blade.

Developement Plan Of Proposed Experimental Facility

The proposed experimental facility will consist of a single, variable pitch, rotating blade with a NACA0015 cross section. The blade will be positioned in the contraction (illustrated in fig.1) of the Department Of Aerospace Engineering's 3ft.x3ft low speed wind tunnel at the University Of Glasgow . As the blade rotates and pitches up, a vortical wake will be generated containing a strong trailed tip vortex. The wake will then convect downstream through the remainder of the contraction and into the working section. This will allow an instrumented blade to be place in the tunnel working section to examine blade-vortex interactions.

To gain some insight into the sizing of the drive and mechanical set-up for the rotor blade a numerical model of the wake produced by the vortex generator has been developed. This has provided valuable information to aid in the mechanical design which is currently underway. Once the vortex generator has been constructed, measurements will be made using hot-wire anemometry to determine the three dimensional convection, strength and geometry of the trailed tip vortex. The measurements will be taken using cross-wire porbes and a TSI Model IFA300 Constant Temperature Anemometer (CTA).

It is important to note that the primary objective of the study is to assess the feasibility of a specific technique for generating a transverse trailed tip vortex. If the facility proves to be successful, BVI studies will then be initiated.

Outline Of Numerical Model.

Introduction

Of particular interest in this study were the relevant geometric parameters and operating conditions of the blade and the wind tunnel to attain a good representation of a transverse vortex. The developed code, therefore, had to be adaptable to enable a comprehensive analysis of fundamental input parameters such as position, size and motion of the blade, and working section velocity. Results had to illustrate the three dimensional developement of the wake (and related tip vortex) through the wind tunnel with enough clarity to isolate the specific effects of a particular design parameter.

The features of the experimental facility that had to be modelled were the vortical wake structure from the rotating blade and the mainstream flow through the wind tunnel. The wake from the rotor was represented by a free wake model consisting of a lattice of shed and trailed vortex elements. The wake was generated using classical lifting line theory which enables the spanwise and temporal changes in bound circulation to be determined and hence the strength of the vortex elements. These elements were then convected through the contraction and working section of the wind tunnel with the superposition of the local velocity, calculated via a three dimensional source panel method, and the induced velocity components from the vortex elements. Due to the inviscid nature of the model no account has been taken for vortex dissipation and so there is no change in the vortex strength with time.

Model Of Wind Tunnel

A source panel method was used to calculate the incompressible, inviscid, potential flow through a low speed wind tunnel. This was based on the work of Hess and Smith[12]. The method was chosen for its relative simplicity and adaptability to internal flows. A considerable amount of theory is available on panel methods[13] and the choice of which to use is determined primarily by the case in question and geometric limitations. Due to the simple geometry of the modelled portion of the wind tunnel and the non-lifting nature of the body, a plane quadrilateral element with constant source distribution was deemed sufficient in this case.

The internal surface of the wind tunnel was discretised into approximately 1000 individual quadrilateral elements representing the Settling Chamber, contraction, working section and diffuser. Since the accuracy of the calculation not only depends on the number of quadrilateral elements used but also on the manner in which these elements are distributed over the surface, a non-uniform distribution of panels was used. In particular, panels were concentrated in the regions of the contraction (area of high curvature) and the working section (area of interest).

Initially, the model requires the specified geometry of the tunnel and from this calculates the corner points of the quadrilateral elements. The control point of each panel, where the fluid velocity normal to the elements is required to vanish (Neumann boundary condition), is then determined. This then allows the induced velocity matrix to be calculated. This induced velocity matrix depends solely on the geometry of the quadrilateral elements and is independent of the onset flow. The matrix contains the components of velocity induced at a point in space by a plane quadrilateral having a constant unit value of source density. This is evaluated for the normal velocities induced by all the quadrilateral elements at each other's control points. Multiplying the normal velocity induced by an element at a particular control

point for a unit source density by the constant but unknown value of the source density on that element, summing over all elements, and repeating for each control point gives the set of total normal velocities at the control point due to the entire approximated body surface. The analytical expressions for this are given in refs. 12,13.

At this stage, the boundary conditions for the surface are now employed. This entails equating the induced normal velocities and the normal components of the onset flow at the control points of the panels to zero. The variation of onset velocity through the wind tunnel, as a result of the changing cross sectional area is obtained be application of the conservation of mass equation based on a specified working section velocity. Once the normal components of this onset flow have been calculated at each control point, the Neumann boundary condition is then applied. This results in a set of linear algebraic equations which is then solved for the required source density distribution using the Gauss-Seidel iterative method.

Once the source density distribution is known the three velocity components at any point in the contraction can be calculated. This is done in exactly the same way as for the induced velocities at the control points i.e. velocities induced by all the panels are calculated, and then added to the local onset flow velocity to get the final total velocity at the prescribed point.

Model Of Rotor Blade and Wake

The model of the rotor blade and wake is based on the work of Coton and Iglesia[9]. Their work was developed to examine how a stream wise convecting vortex interacts with a rotating blade of fixed incidence running at a specified constant blade tip speed. For the present study, it was necessary to remove the convecting vortex and

make provision for variation of the blade incidenceand angular velocity. These features, together with the inclusion of the wind tunnel wall effect, were incorporated by substantial modification of the existing code.

The single blade rotor with a NACA 0015 profile is modelled using a lifting line positioned at the quarter chord line. This line is discretised into several sections and the bound circulation determined via two-dimensional lift curve data fot the aerofoil section. Shed vorticity appears as the variation of the bound circulation with time and trailed vorticity as the difference in circulation between two adjacent spanwise sections. This vorticity is represented in the wake by discrete trailed and shed vortex filaments which are added at each time step. The manner in which these wake filaments move is then determined by a free wake approach. In it, the wake shape is modified at each time step by integration of the velocity field according to the second order Adam's-Bashforth predictor equation. An essential feature of this approach is the calculation of the velocity induced at each node point by all wake filaments and bound vorticity elements. This, together with an increment in the angle of incidence induced at the blade by the wake, is evaluated by application of the Biot-Savart equation.

Within the numerical model, the blade is positioned relative to the wind tunnel co-ordinate system at a location in the contraction. All the rotor and wake calculations are relative to a hub fixed co-ordinate system but are easily transformed into a tunnel fixed co-ordinate system for calculation of the local velocity components. The model allows input specification of azimuthal blade tip velocity and geometric angle of incidence functions. There is also an option to run the blade continuously or for a short period with a specified acceleration/deceleration tip velocity profile. The blade is assumed to be rigid along its span and no allowance has been made for blade flap.

Parameters In The Numerical Model

The numerical model initially reads in an input parameter file which contains all the relevent variables for use in the parametric analysis. The file simplifies alteration of test conditions when running numerous different cases. A discription of the parameters contained within this file is given below.

Blade Axis Position

The rotor blade axis is positioned relative to the wind tunnel co-ordinate system (as indicated in fig.1) whose x-axis lies along the centreline of the tunnel and has the z-axis positive upwards. The origin of tunnel co-ordinate system is located at the entrance to the settling chamber which corresponds to the start of the modelled portion of the tunnel. Although the blade position could be varied in all three co-ordinate directions, only movement in the x-direction was considered in this study. Typical x-values ranged from 2.5 to 3.5 metres relative to the wind tunnel origin.

Blade Geometry

The geometry of the blade is specified by the radius and the chord length. These are primarily determined from the maximum allowable radius available wherever the blade is positioned in the contraction. Values range between 0.8 and 0.55 metres. Changes in chord length provide adjustment of the circulation strength and hence the strength of the trailed tip vortex.

Blade Tip Speed

The blade tip speed can be specified either as a constant for continuous running or as a tip velocity distribution in relation to azimuth. Thus, the blade can be accelerated and decelerated from a specified starting azimuth to a final stopping azimuth.

Working Section Velocity

The working section velocity is specified and used to calculate the required source density. The source density distribution is then used to calculate the local velocities in the wake and on the lifting line due to the wind tunnel geometry. In the study the wind tunnel working section velocity was varied between 10 and 30 m/s which represent the operational limits of the low speed wind tunnel being modelled.

Geometric Angle Of Incidence

The geometric angle of attack is specified at individual azimuthal positions to give an angle of attack distribution for one revolution. For the present application, this involves a pitch-up phase from zero incidence, a constant pitch or ramp down phase to control tip vortex strength and a final pitch down phase to zero incidence. Values up to a maximum of 10 deg were considered although, for the majority of cases, a maximum geometric angle of incidence of 5 degrees produced an adequate tip vortex.

Azimuthal Positions Of Blade

It is necessary to specify a series of motion defining blade positions when the model is used in the acccelerating/decelerating configuration. The specified azimuthal positions correspond to the start and stop positions of the blade and the change over from acceleration to deceleration phases. In this way, three phases of motion can be defined. The first phase consists of an initial acceleration up to a specified tip speed which is sufficient to overcome reversed flow problems. In the second phase, the blade is either accelerated again or held at a constant tip speed. Finally, the blade is decelerated back down to rest.

Rotor Blade Root Cut-Off

To eliminate any numerical instabilities caused by the rotor hub arrangement a root cut-off is required. This is set at 20 % of the rotor radius. In the experimental set-up

this portion of the blade will be taken up by the pitch mechanism and rotor hub, consequently, it will contribute little to the aerodynamic behaviour of the blade.

Wake Core

A Scully vortex was adopted for the vortex elements with the vortex core radius set at 20 % of the blade chord. This corresponds to typical values obtained from experimental measurements carried out at Glasgow University.

Influence Of Vortex Filaments

To enhance computational efficiency, there is a cut-off distance beyond which the influence of a vortex filament is assumed to be zero. This can be varied but a value of two metres was found to be optimum.

Time Step and Duration Of simulation

For a given distance of wake travel, the duration of the simulation is related to the working section velocity, i.e. a slower working section velocity corresponds to a longer simulation time. Similarly, to retain a given level of detail in the rotor wake, the time step is necessarily related to the rotational speed of the blade.

Results

Introduction

In the course of the present study, a large number of possible configurations were considered. In this section selected results are presented to illustrate the main influences on geometric features of the tip vortex and wake. The results are presented in two sections corresponding to the modes of operation of the rotor i.e. the limited azimuthal range and continuous running cases. The figures show the plane of the wake and the tunnel walls as viewed from above. In each case, the blade axis is indicated and the blade rotates in a clockwise direction. Three dimensional views of the wake and tunnel are not presented as the wake lattice was found to exhibit little wander notably the cross sectional plane along which it convected.

Initial tests were conducted to determine the appropriate range of each parameter and to identify numerical instabilities in the model. These tests were carried out with the rotor at a fixed incidence and constant rotational speed. Initial results were poor as a consequence of the wake distribution induced by a strong vortex shed from the impulsively started blade. Further tests were, therefore, conducted using a prescribed variation of blade incidence. Thus, by setting the initial blade incidence value to zero and allowing it to increase thereafter, it was possible to eliminate the strong starting vortex.

Acceleration/Deceleration Cases

The complete set of test cases which were investigated for this operational mode are given in figure 2. These cases are characterised by a specified function of tip speed

versus azimuth which may be sub-divided into three different phases of motion. Firstly, an acceleration at zero incidence brings the blade up to the necessary speed to avoid numerical instabilities associated with reversed flow. This is followed by a constant velocity or second acceleration phase corresponding to the blade crossing the entrance of the working section. Finally, the blade is brought to rest by a deceleration phase at zero incidence. These three phases of motion were initially confined to one revolution to minimise the disturbance which the rotor may have on the tip vortex but it is possible to extend the acceleration and deceleration phases if required. In each case the pitch motion did not have to have the same prescribed azimuthal break-points as the acceleration/ deceleration phases and was independantly prescribed in the input parameter file.

The analysis first concentrated on the variation of blade speed and working section velocity. Figure 4 illustrates one of the first cases examined. The blade tip speed was set at 70m/s using a blade of radius 0.6 metres positioned at 3.3 metres relative to the wind tunnel origin. This corresponds to a blade position close to the working section. The tip speed was held constant through the second phase of motion during which the blade incidence was set at 5 degrees. For this case, the working section velocity was set at 30 m/s which is the highest velocity attainable in the wind tunnel. From the figure, it is noticeable that the wake lattice is fairly sparse as a consequence of the large time step (0.0035 seconds) used in the calculation. This value was chosen purely to minimise computational time in the initial stages of the study. This value is, however, sufficient to provide enough detail to illustrate the effect which the blade speed and tunnel velocity have on the wake geometry. The figure shows that the wake structure is skewed because of its high convection speed. To study perpendicular BVI, a near symmetrical wake structure would be preferred. There are two possible ways of achieving this. It could be done by either increasing the blade tip speed or decreasing the working section velocity. It would be inadvisable to

increase the blade tip speed too much because of mechanical design considerations and so a reduction in the tunnel velocity would be the most appropriate action.

Figure 5 represents a similar case where the working section velocity is reduced to 20 m/s. All other parameters are unchanged from the previous analysis. As can be seen from the figure, the wake is more symmetrical and much less skewed. The tunnel velocity could be reduced further to 10 or 15 m/s but the time taken for the wake to convect through the working section would be higher. With due consideration being given to the practical problem of vortex dissipation with time, it was decided to fix the working section velocity at 20 m/s for future calculations using the same rotor radius.

Although the reduction in wind tunnel operating speed produced a more symmetric wake structure, it was evident that scope still existed to improve symmetry by varying the rotor speed. For thios reason, the next stage in the work was to alter the second phase of the blade motion from the constant tip velocity previously used to a linearly increasing velocity. Figure 6 illustrates one such case. The blade is accelerated up to 50 m/s then accelerated again across the entrance to the working section up to 90 m/s. For this calculation, the time step was decreased to 0.0025 seconds and so there is an increase in the number of vortex filaments in the figure. As before, the motion of the blade was restricted to one revolution during which the blade was pitched up to 5 degrees whilst accelerating, its incidence was then held constant until the blade was pointing approximately downstream, and then it was pitched down to zero degrees. As may be observed in the figure, the changing incidence generated a strong tip vortex on the right side of the wake with weaker tip vortex elements on the left.

As the blade changes from travelling with the flow to moving against it, the relative velocities which it experiences increase as a result of its orientation to the local flow velocity. Consequently, if the blade velocity was held constant across the working

section, there would be a stronger vortex strength on the left side of the wake compared with the right side. It may, therefore be concluded that obtaining a constant tip vortex strength across the working section whilst ensuring that the wake shape is symmetrical is only possible through control of the tip vortex strength by pitching the blade to counter the increase in relative velocities experienced by the blade. Subsequent analysis concentrated on determining this pitching motion profile so a constant tip vortex strength would span the working section.

Figure 7 is typical of results incorporating pitch down motion as the blade crosses the entrance of the working section. Here the blade is still accelerated in the second phase of motion but the final tip velocity is 100 m/s as compared to 90 m/s in the previous example. The blade axis has also been moved slightly forward from 3.3 to 3.45 metres. Since the blade axis has moved further into the contraction in this case, the increase in mainstream velocity at the blade has to be offset by an increase in tip velocity to counter wake skewing. Also, with the blade being positioned further forward and no reduction in the radius, there is less clearance between the blade tip and tunnel wall. This enables the wake to occupy more of the working section and creates a better tip vortex profile. For the case presented, the pitch profile is characterised by an initial increase to 5 degrees followed by a linear reduction to 2.75 degrees as the blade travels across the working section. The incidence is then finally reduced to zero and the blade brought to rest. The tip vortex strength depicted in the diagram is now fairly constant across the width of the tunnel.

In figure 8 a larger blade of 0.75m was located slighlty further back in the contraction at 3.2m. The working section velocity was also reduced to 15m/s to improve the symmetry of the wake. The blade was initially accelerated up to 50m/s and, as in the previous case, accelerated again across the working section but only up to 90m/s before decelerating back to zero. Even though the tip velocity profile was not altered from previous examples, the increase in blade radius did reduce the rotational speed

of the blade. It is pertinent to note that the separation distance between the tunnel walls and the blade tip was small enough in this case that some doubt must be cast on the validity of the potential flow model within this region.

Before conducting the continual running cases, a single rotation case with a blade of 0.65 metres radius positioned at 3.45 metres was examined for a working section velocity of 20 m/s (figure 9). In this case the blade was accelerated up to a tip speed of 50 m/s which was then held constant across the working section before bringing the blade to rest. Once again, the pitching motion comprised an initial pitch-up to 5 degrees, then a reduction to 2.75 degrees across the working section and finally back to zero. Due to the lower resultant velocities incurred on the left side of the diagram by holding the tip velocity constant there is a lower tip vortex strength in this area compared with previous cases. It was evident from this result that the continual running case would not produce as good a transverse vortex as the single rotation but, as discussed later the mechanical advantages of such an arrangement may be significant.

Continual Running Cases

The continual running cases are characterised by a series of wake lattice generated by each revolution of the blade. All continual running configurations are listed in figure 3. The main reason for concidering continuous running is to simplify the design of the actual facility. As in the previous section, it is necessary to determine the optimum position of the rotor and the most appropriate setting for the working section velocity. In this case, however, it is the influence which these have on the separation between each individual convecting wake which is of primary importance.

Figure 10 depicts a continuous running case with a constant tip speed of 50 m/s. All parameters are the same as the previous single rotation case although a larger time step has been used. This was necessary as a result of the increased computational time required to run the simulation over a longer duration together with the increased number of vortex filaments compared with the single rotation cases. The geometry of the lattice in Fig. 10 is consistent with the previous single rotation depicted in Fig. 9. In both cases, the incidence of the blade section varied linearly between 5 degrees and 2.75 degrees as it crossed the working section. This resulted in non-symmetry of the tip vortex strength which was subsequently overcome by keeping the blade incidence constant when crossing the working section. This also had the practical advantage of simplifying the pitch motion profile. It should be noted, however, that this does not, result in the generation of a constant strength trailed tip vortex. An exact function for incidence variation could be calculated for each azimuth position to attain a constant tip vortex strength but this would only result in a highly complex pitch/azimuth profile which would be difficult to implement experimentally.

Further continuous running cases concentrated on blade position. In figure 11 the blade was moved back to 2.5 metres. The diagram shows the distortion that occurs in the wake with the blade so far back in the contraction/settling chamber. This is exactly the same phenomenon that was noted in an earlier single rotation case. As may be observed, lower streamwise velocity in this region of the tunnel necessitates a lower tip velocity speed to avoid interaction of consecutive wakes. The convective velocity has to be high enough to produce an acceptable separation distance between wake formations. An increase in tunnel velocity to 30 m/s is illustrated in Fig. 12 but the resulting wake structure is unacceptable because of the high curvature of the vortex system in the working section.

Figure 13 illustrates the optimum continuous running case examined in this study. The parameters are chosen to reduce the high rotational speeds incurred in previous

cases and so ease the design criteria. A blade of radius 0.75 metres is positioned at 3.2 metres from the origin of the wind tunnel coordinate system which, interestingly, corresponds to the configuration of the best single rotation case. The tip velocity was again set at 50 m/s with a working section velocity of 20 m/s. The separation between tip vortices is approximately equal to the length of the working section and is sufficient to measure the vortex trajectory without significant influence from preceding vortical wake structures.

Discussion

The results indicate that the wake geometry is primarily determined by the wind tunnel velocity, the blade rotational speed and the position of the hub axis. The relative magnitudes of the tunnel velocity and the rotational speed determine the extent to which the wake is skewed, and the hub position dictates the wake curvature and elongation. For the latter, it is important for the blade to be positioned close to the working section to minimise vortex dissipation and to ensure the generation of a well structured vortex with a high local convection velocity. These three parameters are critical irrespective of whether the blade is in a continuous running configuration or following an acceleration/deceleration profile over a specified azimuth range.

There are considerable differences between the single rotation (acceleration/deceleration profile) and the continual running cases. The single rotation configuration is characterised by a continually varying tip velocity profile representing the constant acceleration and deceleration of the rotating blade. This , in the majority of cases investigated, is contained within one revolution. In the numerical model the motion of the blade is represented by three distinct velocity variations. Initially, there is an acceleration from rest up to a specified tip velocity with the blade pitching up. The blade is then either accelerated again across the entrance to the working section or held at a constant tip velocity before deceleration back to rest. The critical phase of the motion is when the blade crosses the working section. Here, the pitch profile is varied to produce a near constant tip vortex strength. If the blade travels at a constant velocity, the incidence of the blade should be approximately constant, but if the blade is accelerated, the blade must be pitched down to balance the higher normal velocities experienced by the blade.

The continuous running configuration, on the other hand, does not require the complicated motion profiles of the single rotation cases. In fact , the blade operates at

constant rotational speed and only a pitch variation has to be specified. The pitching motion of the blade is, however, determined with reference to the same objective as the single rotation cases i.e. the generation of a constant tip vortex strength. With the blade traversing the working section, the magnitude of the normal velocity experienced by the blade is dominated by the component of velocity derived from the rotation of the blade. The local wind tunnel velocity does influence this value but the magnitude of the normal component on the blade from the tunnel is small compared to that of the rotating blade. Hence, it is appropriate to conclude that with an almost constant tip velocity profile in this region a constant pitch incidence would be acceptable to attain (approximately) a constant tip vortex strength.

From the two configurations investigated the results indicate that the best case configuration for the generation of a lateral vortex occurs in the acceleration/ deceleration case. This corresponds to a single rotation consisting of a rapid acceleration up to a tip speed of 50 m/s, followed by an acceleration phase across the working section up to 90 m/s and finally a rapid deceleration back to rest (figure 8) . In this case, the blade radius is 0.75 m and the hub is located at 3.2 m from the wind tunnel origin. To enable the generation of a constant tip vortex strength, the pitch motion of the blade consists of a ramp up to 5 degrees during the initial acceleration phase, followed by a ramp down to 2.75 degrees to balance the higher normal velocities, before the blade is returned to zero incidence during the deceleration phase.

By restricting the motion of the blade to one revolution, extremely high blade accelerations occur. Consequently, any mechanism to actuate the rotor must be able to impose very high torques to attain the prescribed accelerations. One possible way of ameliarating this requirement could be to extend the range of motion over two or more revolutions to reduce the high loads during the initial acceleration and final deceleration phases. Extending these phases does not adversely affect the wake

structure as long as the blade is held at zero incidence during the extended range of motion. The severe accelerations coould also be reduced by either increasing the blade radius or reducing the wind tunnel velocity (which enables a reduction in rotational speeds). The blade radius, however, is restricted by the contraction geometry and a reduction in tunnel velocity is not advisable due to the need for the vortex to have a high convection velocity. Unfortunately, there is no practical solution to reduce the extremely high loads in the critical phase when the blade is accelerating across the entrance to the working section.

In the continuous running cases the wake geometry is not significantly different to that produced in the corresponding single rotation acceleration/deceleration cases when the tip velocity is held constant across the working section (figs.9,10). Since, however, the blade now operates with a constant tip velocity around the azimuth, consideration focuses on the separation between the consecutive wake structures generated by each revolution rather than to what extent the wake geometry is skewed. This separation distance is dependant on the relationship between wind tunnel velocity and blade tip velocity. These, together with the rotor hub position, also determine the geometric features of the wake.

The design criteria for the rotating blade are considerably simpler for the continual running case. Since there are no stringent limitations with repect to blade travel, the blade could be run up to speed over a number of revolutions then left to wind-down after measurement. This would result in a considerable reduction in the loads required to rotate the blade.

There is no significant difference between the physical dimensions and position of the rotating blade in the best case continual running and single rotation cases. The difference between the two arises from the type of actuation that would be required to produce the torque for either the short period variable acceleration motion or the

long duration constant velocity motion. It is interesting to note that the tip speed of 50 m/s and radius of 0.75m corresponds to approximately 11 revolutions per second which is marginally higher than the 9 revolutions per second of the current Glasgow University BVI facility. That facility is driven by a geared down servo motor and has a larger blade with a higher inertia than the proposed rig. It should, therefore, be possible to utilise the existing motor or one similar as the actuation for the proposed facility if the continuous running mode were adopted. Initial estimates would indicate that for the acceleration/deceleration configuration, a hydraulic system, which would be prohibitively expensive, would be required to produce the prescribed motion profile over two revolutions. Since the geometry of the vortex structure is not significantly worse in the continual running configuration it would be difficult to justify the added expense that would be required to implement the acceleration/deceleration case.

The pitching motion of the blade would also be achieved more easily with the blade in the continuous running configuration. A prescribed incidence variation could be obtained using a simple swash-plate mechanism. This would provide the periodic wake generation depicted in the results. Another option may be to incorporate a motor within the hub. Whilst this would provide ease of control and adaptability to different pitch profiles, it would inevitably be more difficult to implement and incur higher costs. This would be unavoidable if the short period acceleration/deceleration mode was implemented as the optimum prescribed pitch profile is non-periodic.

Practical consideration must also be given to the proximity of the blade tip to the tunnel wall during the rotation of the blade. The numerical model takes no account of the viscous effects that would be experienced in this region. This is not a feature when the blade crosses the working section but must be considered when the blade initially pitches up to generate the wake. Viscous interaction with the wall may result in vortex dissipation and produce unwanted phenomena in the convecting vortex

structure. If this does occur then alteration of the radius of the blade would probably be required.

Conclusions

A numerical model has been used in the conceptual design of a new blade vortex interaction facility. The model showed the convecting wake geometry was dependant on the wind tunnel velocity, the tip velocity profile and the pitching motion of the rotating blade. Two independent cases for the motion of the blade were investigated, a single rotation acceleration/deceleration motion and a continuous running motion with constant tip velocity. The single rotation case, with an acceleration across the entrance to the working section , produced the optimum wake geometry for the generation of a lateral vortex but may be impractical to implement due to the excessively high torques required to accelerate and decelerate the blade. The continuous running configuration produces a wake geometry which is not significantly worse than the single rotation case but would have the advantages of being considerably easier to implement.

Further Work

This will involve the design and construction of the facility and subsequent measurement of the convecting trailed tip vortex. Construction will be based on the continuously rotating blade configuration . The hot-wire measurement system will be set-up and initial calibration and bench mark tests will be conducted.

References

1. Surendraiah, M. "An Experimental Study of Rotor Blade-Vortex Interaction.", M.S. Thesis, The Pennsylvaia State University, December 1969.

2. Padakannaya, R. "Experimental Study of Rotor Unsteady Airloads due to Blade-Vortex Interaction.", NASA CR-1909, November 1971.

3. Caradonna, F.X., Lautenschlager, J.L., Silva, M.J., "An Experimental Study of Rotor-Vortex Interaction." AIAA Paper 88-0045, AIAA 26th Aerospace Sciences Meeting, Reno, Nevada, Jan 1988.

4. Horner, M.H., Saliveros, E., Galbraith, R.A.McD., "An Experimental Investigation of the Oblique Blade-Vortex Interaction.", 17th European Rotorcraft and Powered Lift Aircraft Forum, Berlin, Germany, Sept 1991.

5. Horner, M.H., Saliveros, E., Galbraith, R.A.McD., "An Examination of Vortex Convection Effects During Blade-Vortex Interaction.", AHS/RAeS Technical Specialists Meeting on Rotorcraft Acoustics and Rotor Flight Dynamics, Philadelphia, U.S.A.,Oct 1991.

6. Horner, M.H., Stewart, J.N.,, Galbraith,R.A.McD., Grant, I., Coton, F.N., Smith, G.H. "Preliminary Results from a Particle Image Velocimetry Study of Blade-Vortex Interaction." 19th European Rotorcraft Forum, Cernobbio, Italy, Sept 1993.

7. Seath, D.D., Kim, J.M., Wilson, D.R. "An Invesigation of the Parallel Blade-Vortex Interaction in a Low-Speed Wind Tunnel.", AIAA Paper 87-1345, 19th Fluid Dynamics, Plasma Dynamics and Lasers Conference, Honolulu, Hawaii, June 1987.

8. Straus, J., Renzoni, O., Mayle, R.E. "Airfoil Pressure Measurements During a Blade-Vortex Interaction and Comparison with Theory.", AIAA Paper 88-0669, 26th Aerospace Sciences Meeting, Reno, Nevada, Jan 1988.

9. Coton, F.N., De la Iglesia, F. "A Three-Dimensional Model Of Low Speed Blade-Vortex Interaction." 20th European Rotorcraft Forum, Amsterdam, Oct 1994.

10. Wall, B.G., van der "CP-ROT, First Results from Pressure Instrumented BO-105 Hingeless Model Rotor Tests" 19th European Rotorcraft Forum, Cernobbio, Italy, Sept 1993.

11. Ellin, A.D.S. "An In-Flight Investigation of Lynx AH MK5 Main Rotor/Tail Rotor Interactions.", 19th European Rotorcraft Forum, Cernobbio, Italy, Sept 1993.

12. Hess, J.L.,Smith, A.M.O. "Calculation of Potential Flow About Arbitrary Bodies." Progress in Aeronautical Sciences, vol. 8, pp. 1-138 , 1967.

13. Katz, J., Plotkin, A. "Low-speed Aerodynamics-From Wing Thoery to Panel Methods."McGraw-Hill Publications Inc., 1991

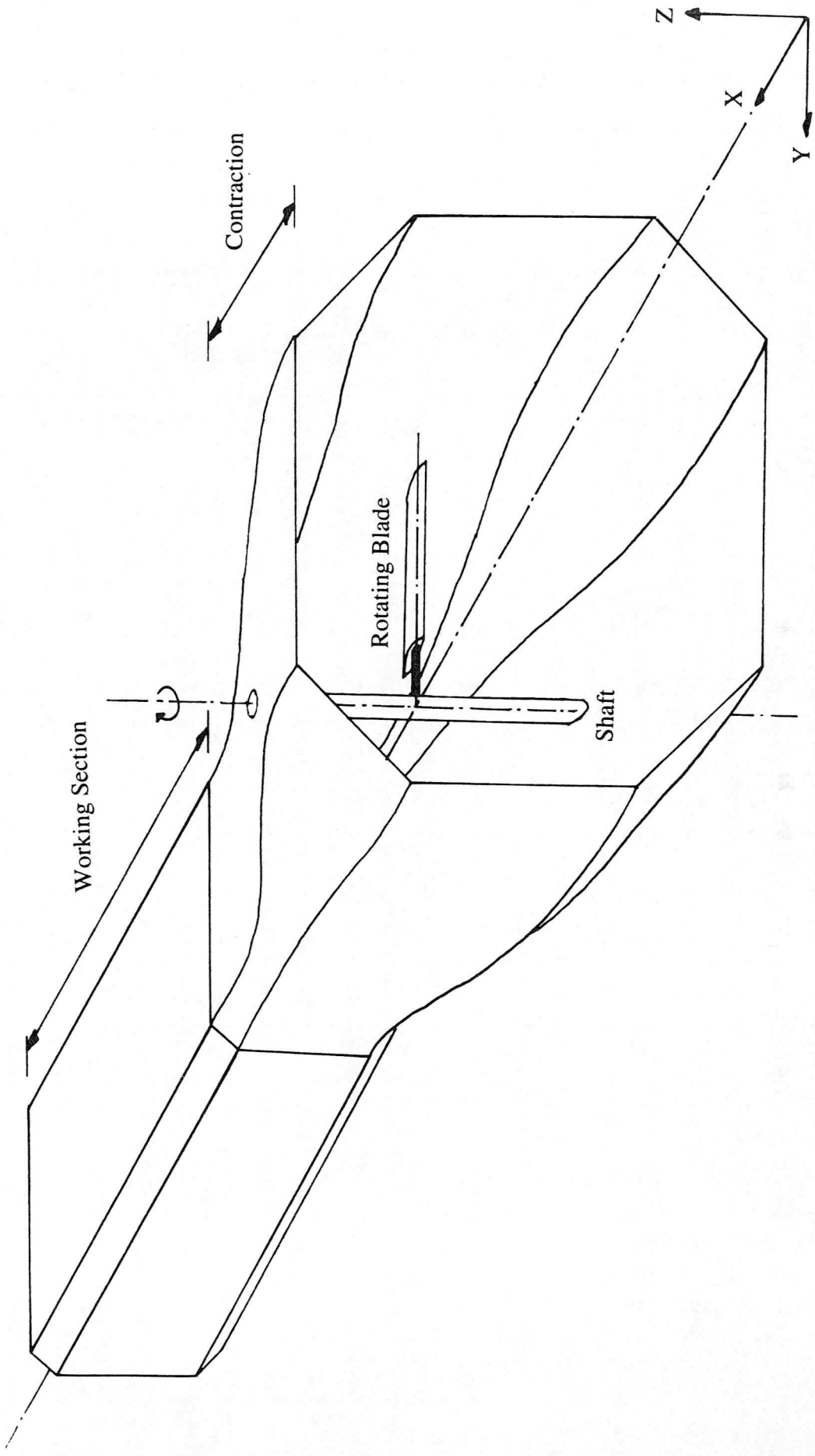

Fig.1 Diagram of experimental set-up indicating the wind tunnel co-ordinate system.

Case	AOA1	AOA2	c	R	X	Y	Start Azi	AZI1	AZI2	Stop Azi	Start Alp	ALP1	ALP2	Stop Alp	WS Vel	TV1	TV2	tmax	tstep	nplot
1	5	5	0.09	0.7	3	0	225	300	420	500	270	315	390	450	20	70	70	0.15	0.0035	15
2	5	5	0.09	0.6	3.3	0	225	300	420	500	270	315	390	450	20	70	70	0.15	0.0035	13
3	5	5	0.09	0.6	3.3	0	225	300	420	500	270	315	390	450	30	70	70	0.15	0.0035	15
4	5	5	0.09	0.6	3.3	0	225	300	420	500	270	315	390	450	30	50	70	0.17	0.0035	20
5	5	5	0.09	0.6	3.3	0.1	225	300	420	500	270	315	390	450	30	50	70	0.17	0.0035	20
6	5	5	0.09	0.6	3.3	0	225	300	420	500	270	315	390	450	20	50	70	0.2	0.0035	20
7	5	5	0.09	0.6	3.3	0	225	300	420	500	270	315	390	450	20	50	90	0.2	0.0035	20
8	5	5	0.09	0.6	3.3	0	225	300	420	500	270	315	390	450	25	50	90	0.2	0.0035	15
9	5	5	0.09	0.6	3.3	0	180	270	345	500	270	315	350	400	25	50	90	0.2	0.0035	15
10	5	5	0.09	0.6	3.3	0	180	270	345	500	270	315	350	450	20	50	90	0.2	0.0035	20
11	5	5	0.09	0.6	3.3	0	180	270	370	500	270	315	350	450	20	50	90	0.2	0.0025	20
12	5	5	0.09	0.6	3.3	0	180	270	390	500	270	315	350	450	20	70	110	0.2	0.0025	20
13	5	5	0.09	0.6	3.3	0	180	300	390	500	270	315	350	450	20	50	100	0.2	0.0025	20
14	5	5	0.09	0.55	3.3	-0.2	180	300	390	540	270	315	350	450	20	50	100	0.2	0.0025	20
15	5	5	0.09	0.6	3.3	0	180	300	390	540	250	300	405	540	20	50	100	0.2	0.0025	20
16	5	5	0.09	0.6	3.3	0	180	300	390	540	250	300	405	540	20	50	100	0.2	0.0025	20
17	5	5	0.09	0.6	3.3	0	180	300	390	540	250	300	450	540	20	50	100	0.2	0.0025	20
18	5	5	0.09	0.6	3.2	0	180	300	390	540	250	300	450	540	20	50	100	0.2	0.0025	20
19	5	2	0.09	0.6	3.2	0	180	300	390	540	250	300	390	540	20	50	100	0.2	0.0025	20
20	5	2.5	0.09	0.6	3.3	0	180	300	390	540	250	300	390	540	20	50	100	0.2	0.0025	20
21	5	3	0.09	0.6	3.4	0	180	300	390	540	250	300	390	540	20	50	100	0.2	0.0025	20
22	5	2.75	0.09	0.6	3.45	0	180	300	420	540	250	300	390	490	20	50	100	0.2	0.0025	20
23	5	2.75	0.09	0.6	3.45	0	180	300	440	540	250	300	390	490	20	50	100	0.2	0.0025	20
24	5	2.75	0.09	0.6	3.45	0	0	300	440	720	250	300	390	490	20	50	100	0.4	0.0035	20
25	5	2.75	0.09	0.6	3.45	0	180	300	420	540	250	300	390	490	15	60	100	0.2	0.0025	20
26	5	2.75	0.09	0.6	3.45	0	180	300	420	540	250	300	390	490	20	60	100	0.2	0.0025	20
27	5	2.75	0.09	0.8	3	0	180	300	420	540	280	320	400	450	20	30	60	0.4	0.0035	20
28	10	5	0.09	0.6	3.45	0	180	300	420	540	280	330	400	450	20	50	100	0.2	0.0025	20
29	5	2.75	0.09	0.75	3.2	0	180	300	420	540	280	330	400	450	20	50	90	0.2	0.0025	20
30	5	2.75	0.09	0.75	3.2	0	180	300	420	540	280	330	400	450	15	50	90	0.35	0.003	20

Fig.2 Table of acceleration/deceleration cases.

Case	AOA1	AOA2	c	R	X	Y	Start Azi	AZI1	AZI2	Stop Azi	Start Alp	ALP1	ALP2	Stop Alp	WS Vel	TV1	TV2	tmax	tstep	nplot
31	5	2.75	0.1	0.6	3.45	0	0	300	420	730	250	330	380	490	20	50	50	0.3	0.0025	20
32	5	2.75	0.1	0.6	3.45	0	0	300	420	730	250	330	380	440	20	35	50	0.2	0.0015	20
33	5	2.75	0.1	0.6	3.45	0	0	300	420	730	250	330	380	440	20	50	50	0.2	0.0015	20
34	5	2.75	0.1	0.65	3.45	0	0	300	420	730	250	330	380	440	20	50	50	0.2	0.0015	20

Fig.2 Table of acceleration/deceleration cases (continued).

Case	AOA1	AOA2	c	R	X	Y	Start Azi	AZI1	AZI2	Stop Azi	Start Alp	ALP1	ALP2	Stop Alp	WS Vel	TV1	TV2	tmax	tstep	nplot
35	5	2.75	0.15	0.65	3.45	0	0	-	-	-	250	330	380	440	20	50	-	0.4	0.0025	20
36	5	2.75	0.15	0.7	3	0	0	-	-	-	250	330	380	440	20	50	-	0.4	0.0025	20
37	5	2.75	0.15	0.8	2.5	0	0	-	-	-	250	330	380	440	20	50	-	0.3	0.0035	20
38	5	2.75	0.15	0.8	2.5	0	0	-	-	-	250	330	380	440	30	50	-	0.3	0.0035	20
39	5	2.75	0.15	0.75	3.2	0	0	-	-	-	250	330	380	440	30	50	-	0.3	0.003	20
40	5	2.75	0.15	0.75	2.8	0	0	-	-	-	250	330	380	440	30	50	-	0.3	0.003	20
41	5	2.75	0.15	0.75	2.8	0	0	-	-	-	250	330	380	440	20	50	-	0.3	0.003	20
42	5	2.75	0.15	0.75	3.2	0	0	-	-	-	250	330	380	440	20	50	-	0.3	0.003	20
43	5	2.75	0.09	0.75	3.2	0	0	-	-	-	250	330	380	440	20	50	-	0.3	0.003	20
44	8	4	0.09	0.75	3.2	0	0	-	-	-	250	330	380	440	20	50	-	0.3	0.003	20
45	10	5	0.09	0.75	3.2	0	0	-	-	-	250	330	380	440	20	50	-	0.3	0.003	20
46	10	10	0.09	0.75	3.2	0	0	-	-	-	250	330	380	440	20	50	-	0.3	0.003	20
47	5	5	0.15	0.75	3.2	0	0	-	-	-	250	330	380	440	20	50	-	0.3	0.003	20
48	10	10	0.15	0.75	3.1	0	0	-	-	-	250	330	380	440	20	50	-	0.3	0.003	20
49	5	5	0.15	0.75	3.1	0	0	-	-	-	250	330	380	440	20	50	-	0.3	0.003	20
50	5	5	0.09	0.75	3.1	0	0	-	-	-	250	330	380	440	20	50	-	0.3	0.003	20

Fig.3 Table of continuous running cases.

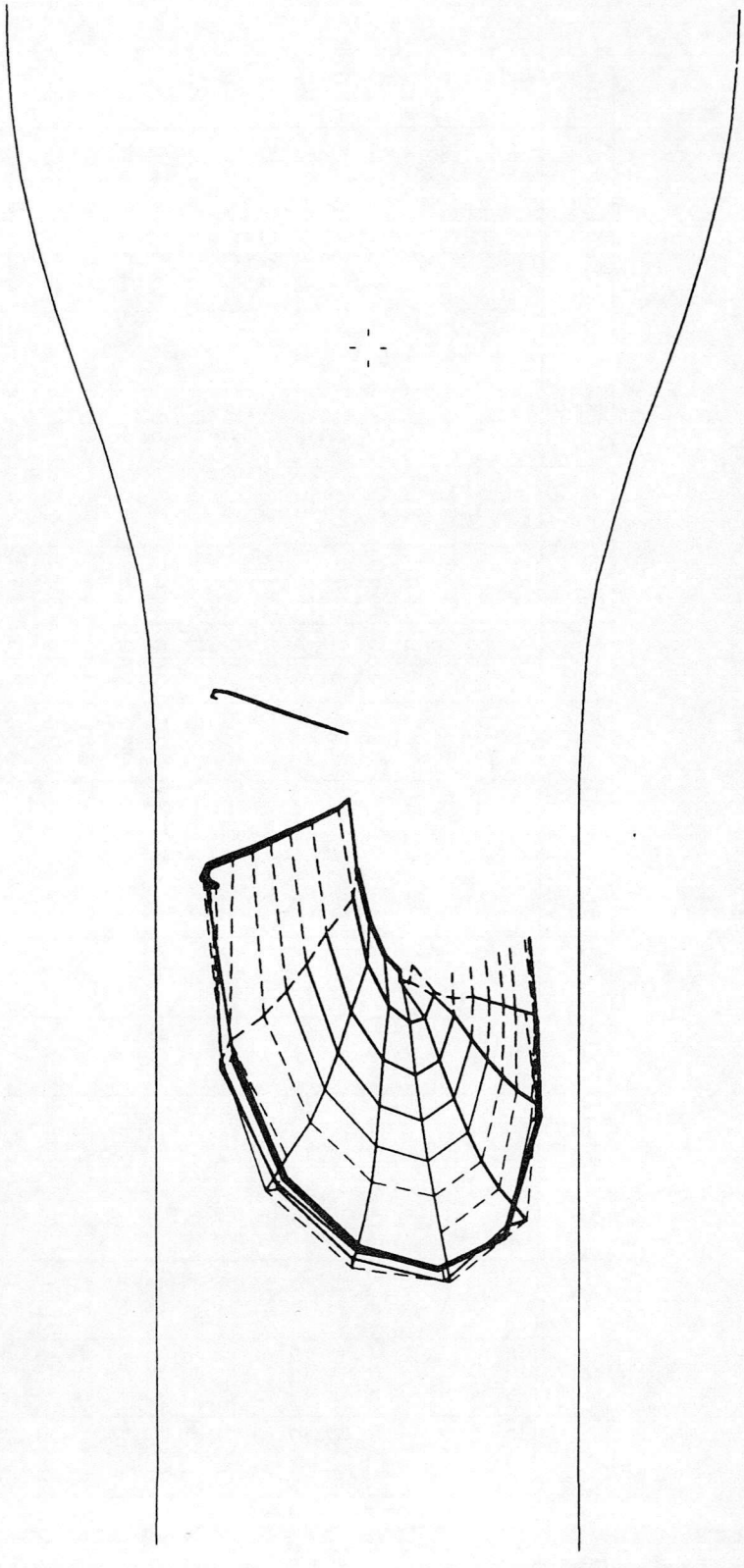

Fig.4 Single rotation convecting wake with working section velocity at 30 m/s, tip velocity constant at 70 m/s across working section.

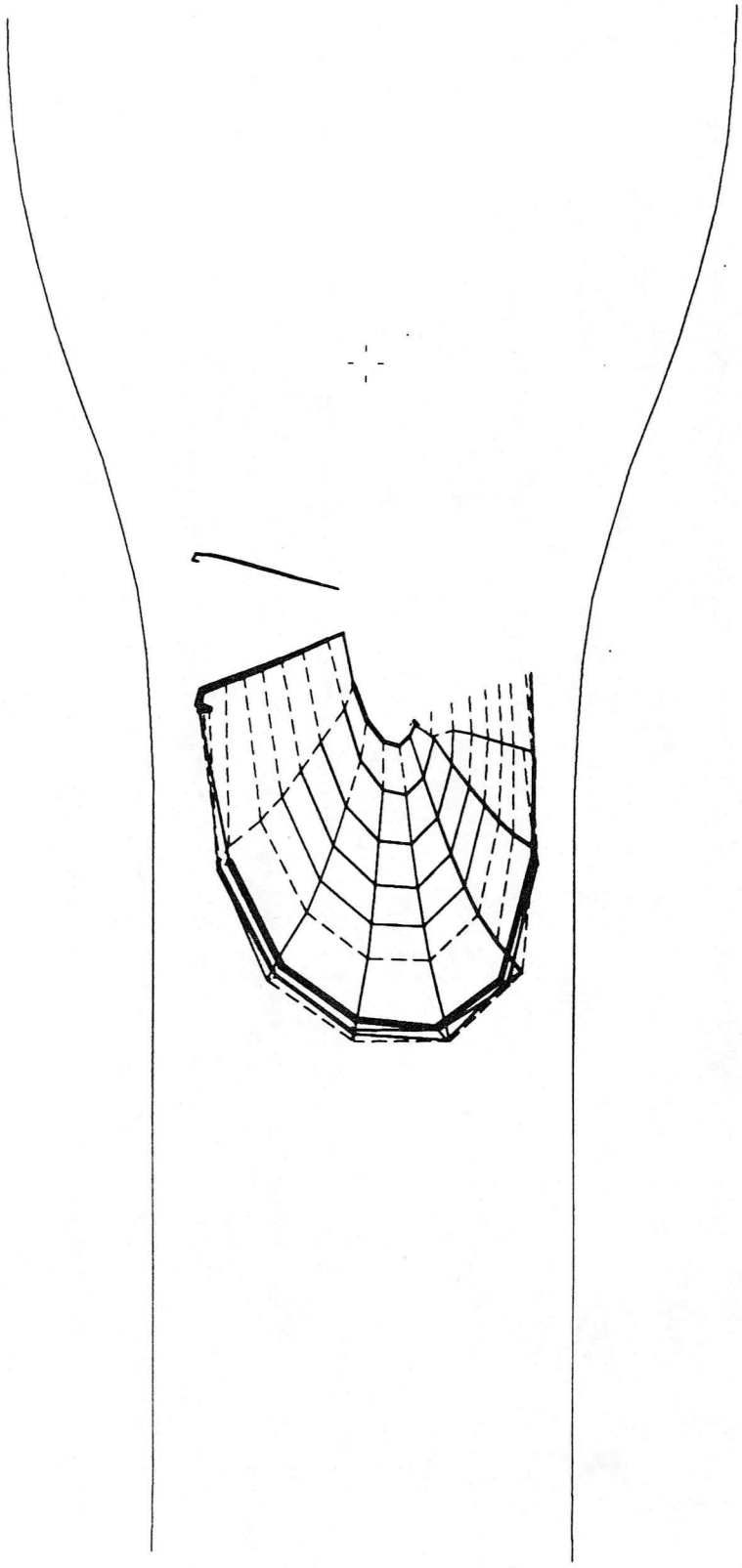

Fig.5 Single rotation convecting wake with working section velocity at 20 m/s, tip velocity constant at 70 m/s across working section.

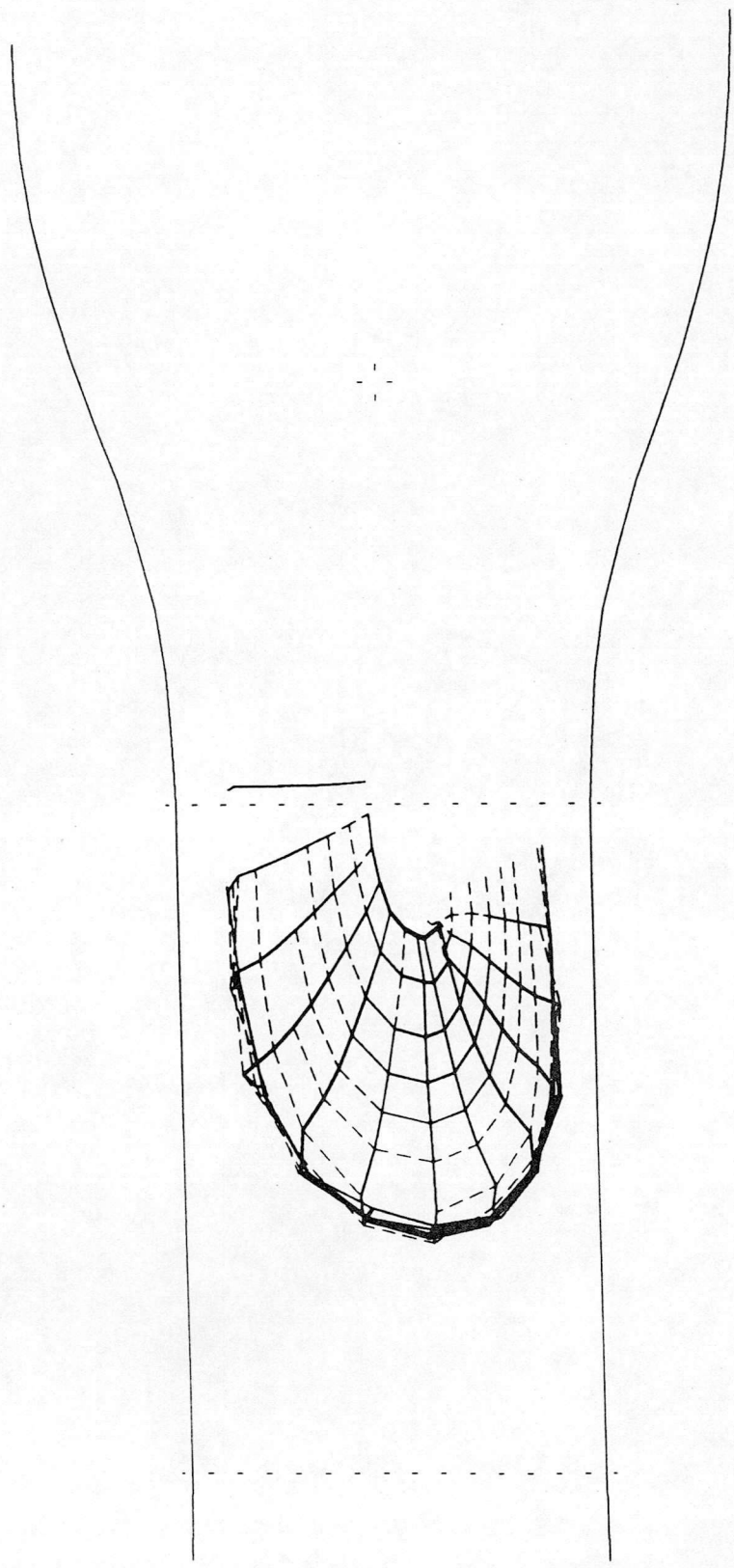

Fig.6 Single rotation convecting wake with working section velocity at 20 m/s, tip velocity increasing from 50 m/s to 90 m/s across working section, incidence held constant at 5 deg.

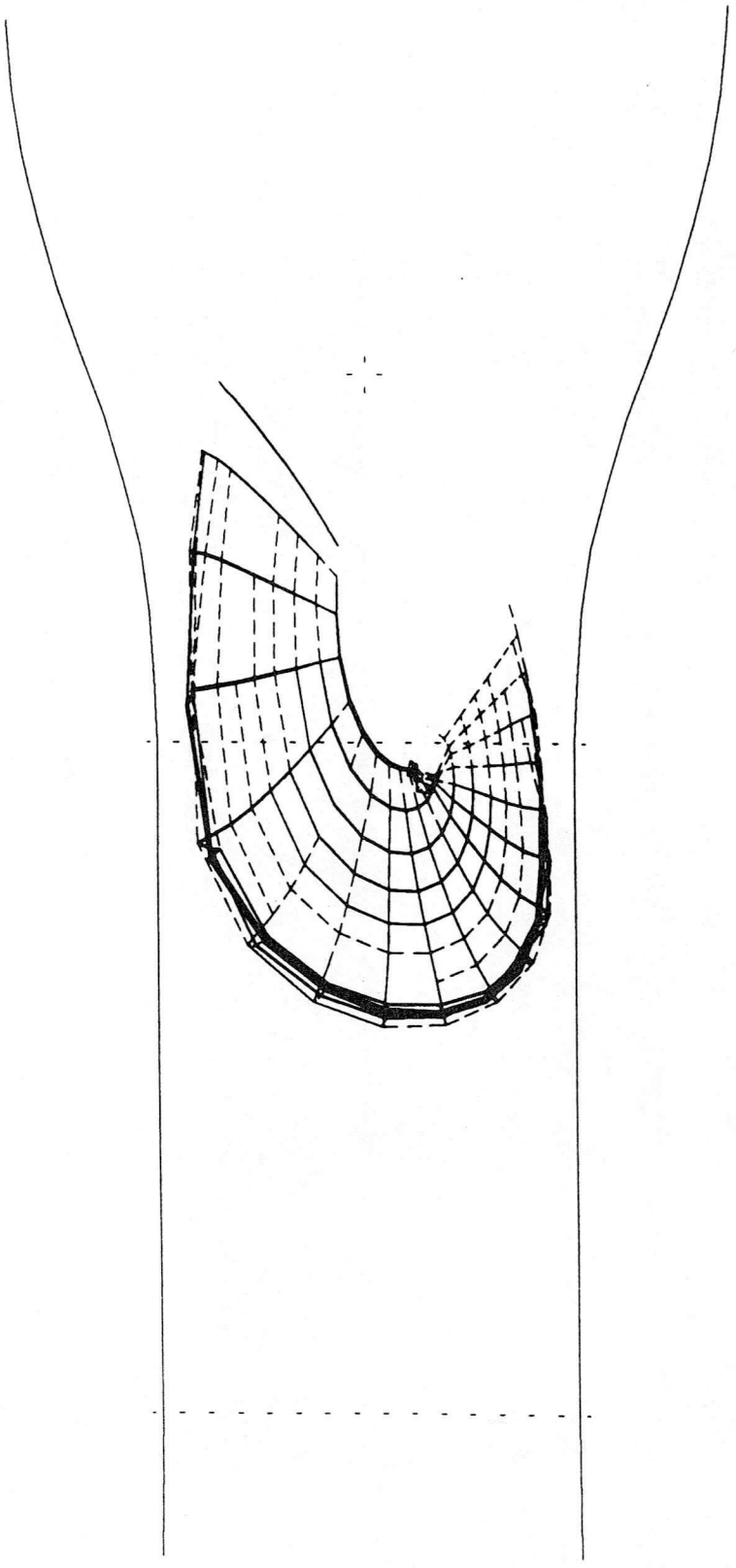

Fig.7 Single rotation convecting wake, tip velocity increasing from 50 m/s to 90 m/s across working section with pitch down from 5 deg. to 2.75 deg.

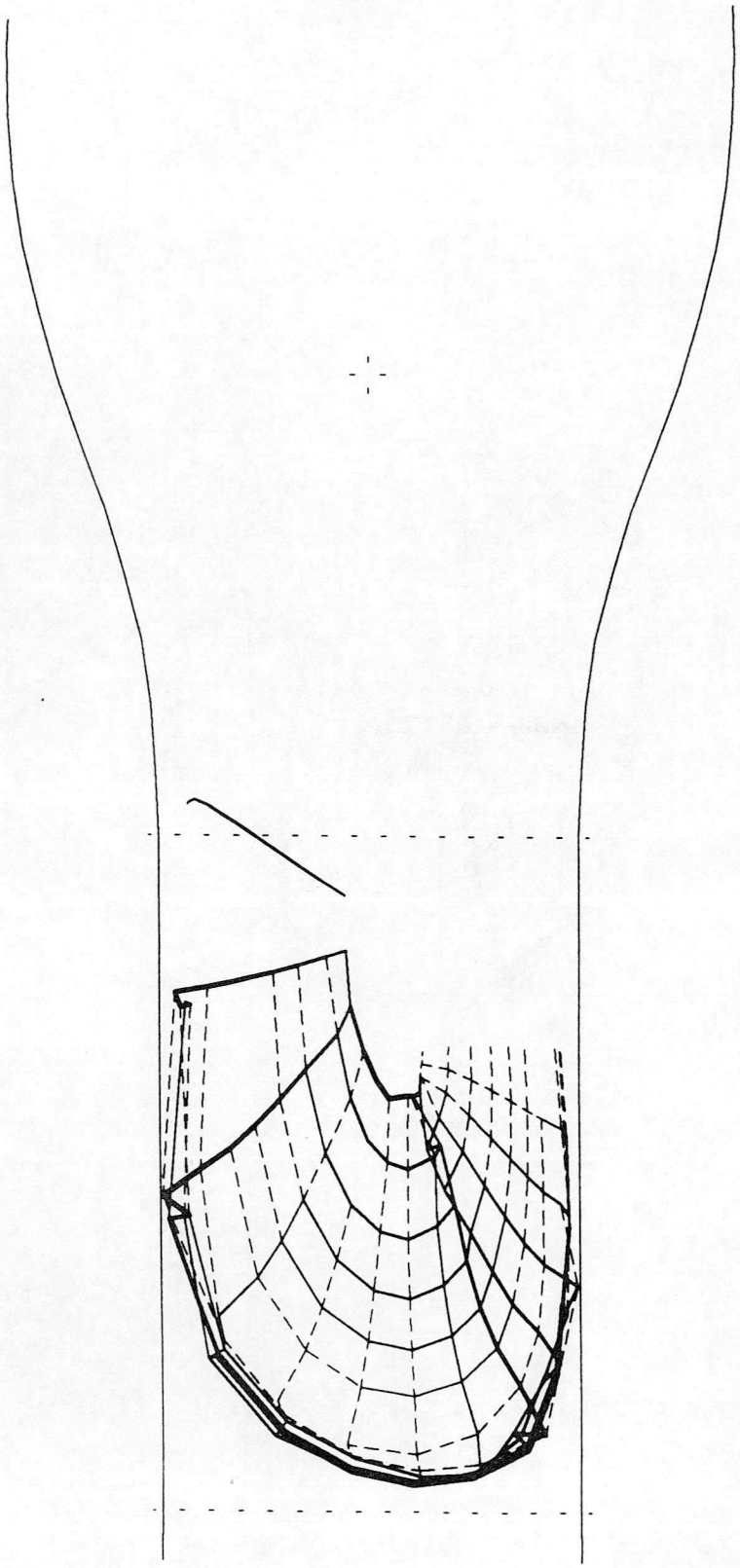

Fig.8 Single rotation convecting wake with a blade of radius 0.75m positioned at 3.2m from tunnel origin, working section velocity 15m/s.

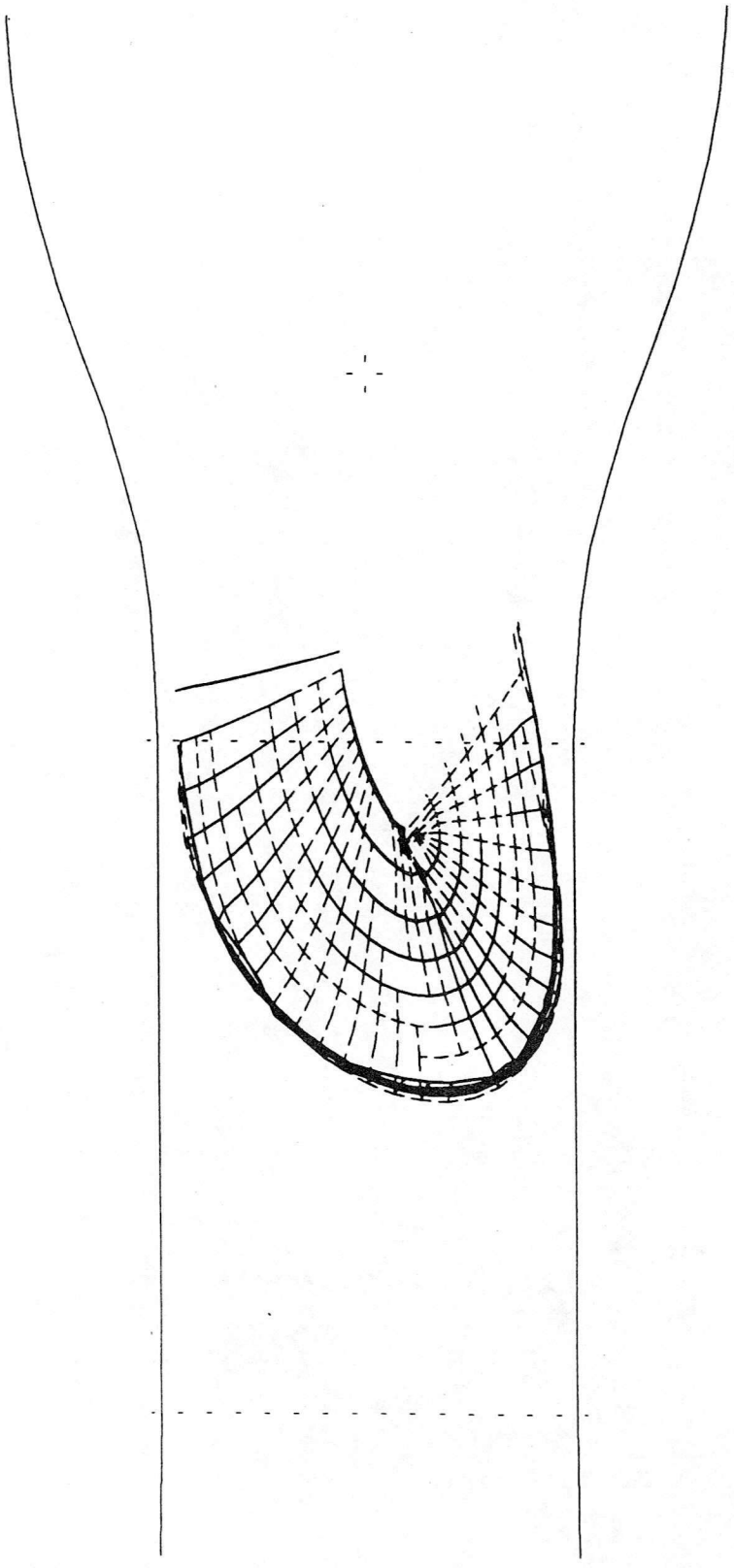

Fig.9 Single rotation convecting wake with tip velocity constant at 50 m/s across working section, blade radius 0.65m positioned at 3.45m from origin.

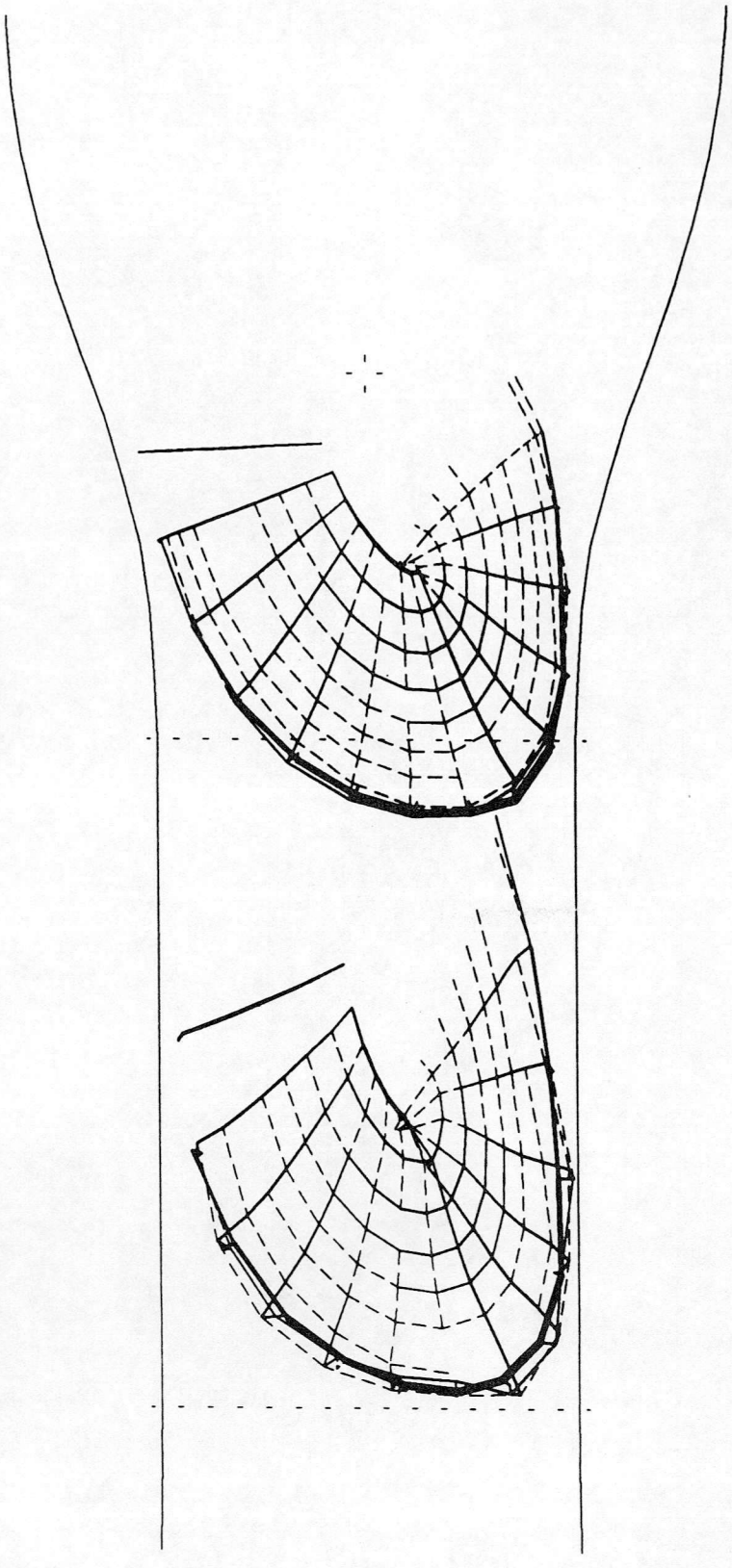

Fig.10 Continuous running wake development with a blade of radius 0.65m positioned at 3.45m from tunnel origin.

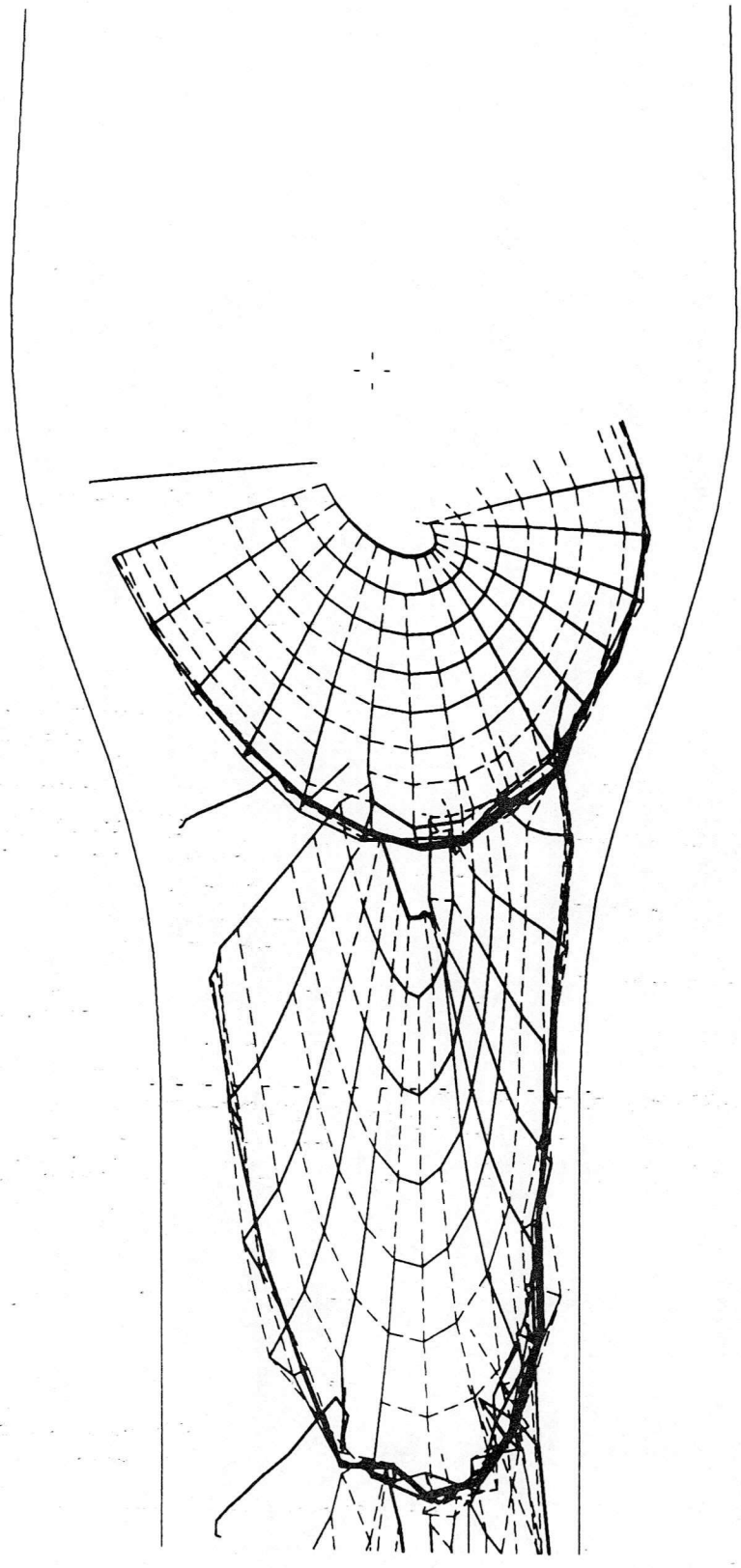

Fig.11 Continuous running wake development with a blade of radius 0.8m positioned at 2.5m from tunnel origin, working section velocity 20 m/s.

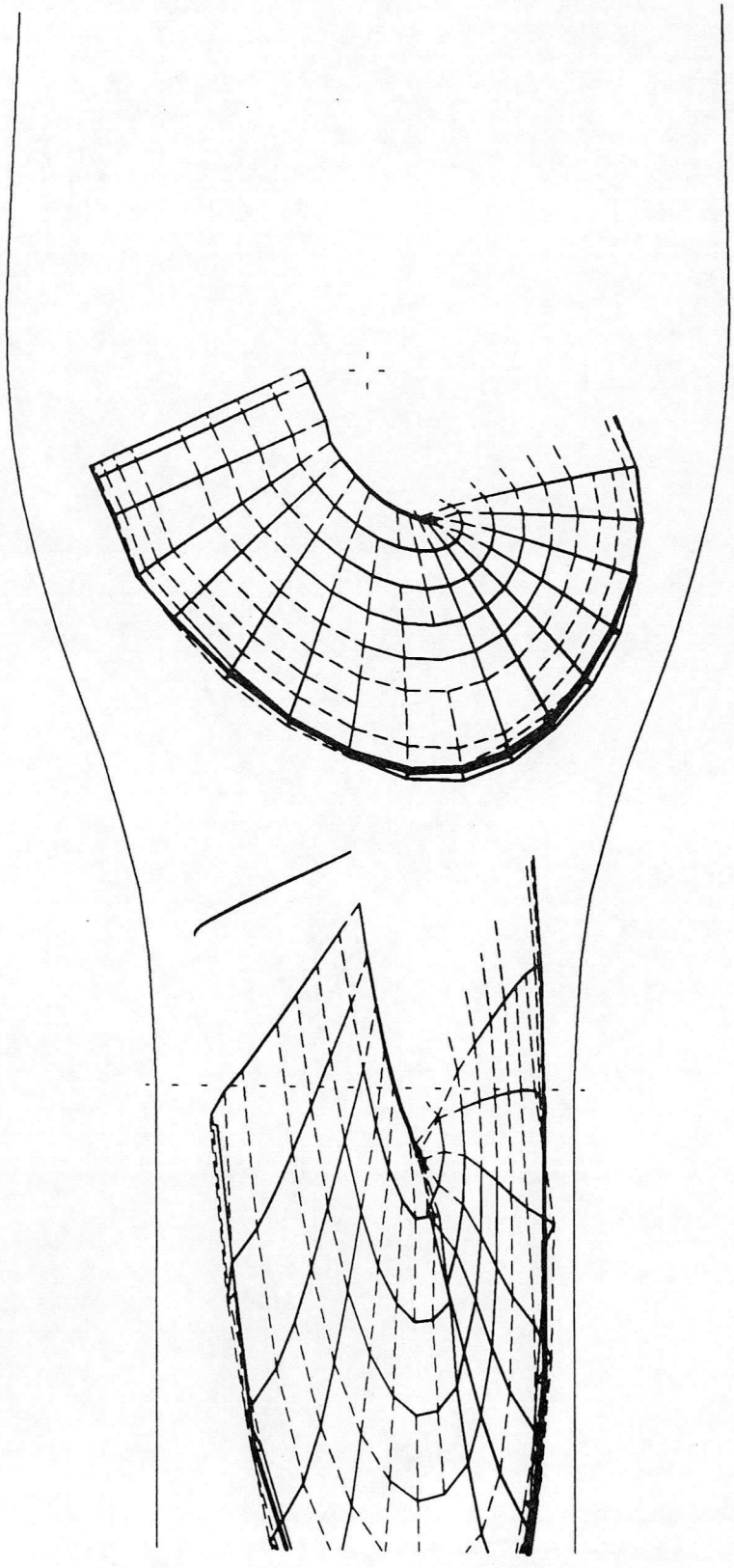

Fig.12 Continuous running wake development with a blade of radius 0.8m positioned at 2.5m from tunnel origin, working section velocity 30m/s.

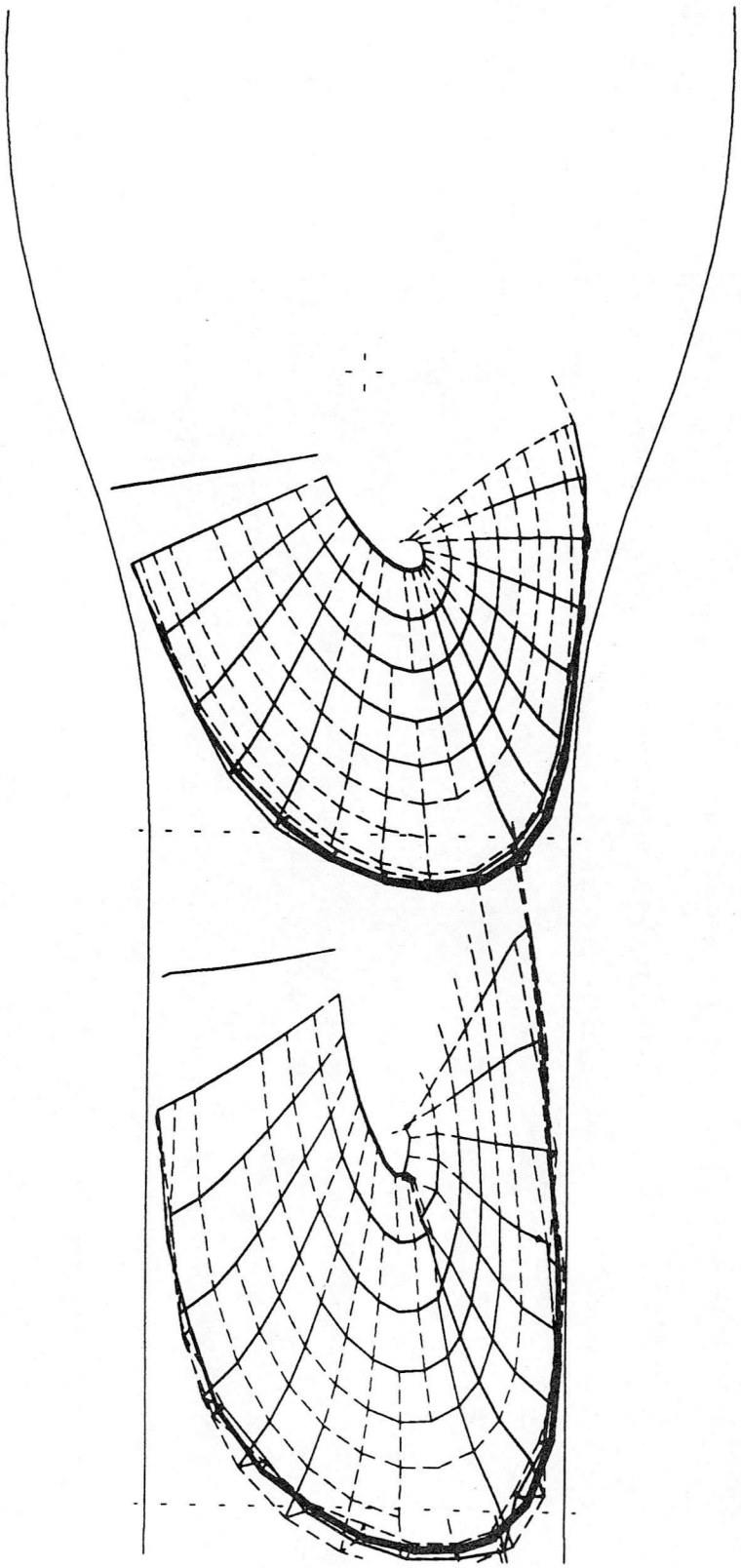

Fig.13 Continuous running wake development with a blade of radius 0.75m positioned at 3.2m from tunnel origin.